

# **Low-Cost 10 kW Inverter System for Fuel Cell Interfacing Based on PWM Cycloconverter**

Philip Krein                  Robert Balog                  Leanne Cerven                  Nate Schweigert  
Nick Schroeder                  Jason Woodard                  Brian Mathis

University of Illinois at Urbana-Champaign

Department of Electrical and Computer Engineering

1406 West Green Street

Urbana, Illinois 61801

Phone: (217) 333-4732                  Fax: (217) 333-1162                  E-mail: [machines@ece.uiuc.edu](mailto:machines@ece.uiuc.edu)

## **Contents**

1. Introduction
2. Topology – general issues
3. Topology – specifics
4. Filtering
5. General tradeoffs and auxiliary design issues.
6. Control
7. Simulation and experiment
8. 1500 W prototype
9. Cost analysis
10. Education and the team
11. Operating instructions
12. References

## *Abstract*

A low-cost high-performance sinusoidal inverter for nominal 48 V dc to 120 V ac conversion is described. The design minimizes overall system cost – including energy storage and management. The design provides low-ripple current-controlled interfacing to the fuel-cell stack, an intermediate-voltage battery energy storage buffer, and an ac-link output inverter. The circuit is based on square-wave cycloconverter technology, combined with a simple approach that produces a patent-pending “PWM cycloconverter” modulation process. The approach keeps the number of stages and magnetic elements low while providing galvanic isolation. Either SCRs or IGBTs can be used as output devices, which provides an unusual cost/performance trade-off possibility. Gate drives and other control elements are also simplified. The design provides excellent performance with a minimum of filter components and a simple control. Fuel-cell current is controlled with a long-term moving average method. This assures that the batteries are kept nearly full at all times with minimal sensing and control overhead.

## **1. Introduction**

Fuel cells combine hydrogen (or other oxidizable fuel), oxygen, and an ionic conductor electrolyte to produce electrochemical oxidation. The results are oxidized fuel – such as water – and electric current. Because the reactions are electrochemical rather than thermal, the energy conversion efficiency can be very high. The operation is similar in many ways to that of a battery. The primary exception is that a continuous fuel source is provided to keep the reactions going indefinitely [1].

The 2001 Future Energy Challenge teams were given the objective of designing low-cost power interfaces that can convert dc power from a fuel cell into conventional ac power for use in a home or business. The design requirement is to deliver up to 10 kW in a design that can be manufactured for a cost less than \$0.05 per watt. This cost is much lower than those achieved by fuel cell system vendors to date, and is somewhat lower than levels achieved by vendors of backup power inverter systems.

One challenge with a fuel cell is that the reaction rate is controlled in part by delivery of fuel. The fuel must be delivered at least as fast as it is consumed, but fuel is wasted if the delivery rate is faster. In a practical system, this means that a fuel cell looks like a battery with very slow dynamics: the time rates of change associated with sensors, pumps, fans, and the system exhaust means that the fuel cell controller requires approximately one minute to respond to a command for change, and about 90 s for initial start. In an inverter system, the ac side load will have dynamics much faster than this, so an energy storage buffer will be necessary.

At a given fuel flow rate, a fuel cell has an optimum output current – that current that will provide the highest output power while minimizing losses and internal wear and tear. This behavior is somewhat similar to that of a solar cell [2], although it is usual to operate a fuel cell at a current slightly below its maximum power output point to keep reliability high. In the end, current optimization means that a precise average current control is needed for the fuel cell itself.

Fuel cells produce relatively low voltage – a fraction of a volt per cell – since the voltage is related to the electrochemical potential of an  $H_2 - O_2$  reaction. It is possible in principle to draw energy directly from an individual cell. But the realities of device voltage drops and extreme currents mean that a single cell does not provide efficient energy conversion. To alleviate this limitation and to achieve practical voltage levels, many cells must be connected in series. This gives rise to the complete “fuel cell stack.” In general, any voltage can be achieved by stacking cells in series, but in the event of a single-cell failure or degradation, the entire stack will be affected. Thus there is an “optimum voltage” with some cells in series (but not too many). Although this optimum voltage has not been studied rigorously as yet, conventional battery and solar cell practice suggests a level from 20 V to 60 V as a realistic value. The Future Energy Challenge chose a nominal 48 V cell stack as the input to reflect this expectation.

System electrical safety is an issue. However, since it is possible to provide a safe enclosure for a unit, electrical safety is somewhat secondary. Most standards practice accepts dc voltages under 60 V as a

safe level not subject to special protection requirements. On this basis, a 48 V fuel cell stack has important advantages – the open-circuit output when pumps and other necessary hardware are in place is unlikely to exceed 60 V. It is relatively easy to assemble a 48 V fuel cell stack into a system that is safe enough for residential use.

A 48 V output is not enough to achieve a useful ac output voltage. Therefore a step-up function will be required. The only way to achieve highly efficient energy conversion from 48 V dc to conventional 120/240 V ac is to use the techniques of power electronics – switching devices and energy storage elements to perform dc to ac conversion. However, the objective of this project is not just to make power electronic circuits, but also to make them at low cost and to give them high reliability. We consider several issues to meet the requirements at low cost:

1. Keep the circuits as simple as possible.
2. Take advantage of the known dc input and the fixed-frequency ac output. There is no need for extra cost to handle unforeseen inputs and outputs.
3. Use control ideas that do not require special sensors or complicated software.
4. Think about cost at every level. Power losses mean larger, more expensive heat sinks. Features cost money. Dials, displays, and other niceties might not help the user very much. The system might work better with extra batteries, but these are costly and need a lot of care.
5. In most cases, passive parts are cheaper than active parts of similar power rating.
6. A good design that works well is better than a “great” design that does not work.

To achieve an output of 240 V ac (RMS), a dc voltage on the order of  $240\sqrt{2}$  is needed, or nearly 340 V. In any inverter system design, a step-up function from 48 V to 340 V will be needed. One additional challenge is that current levels can be high in a 48 V system. Consider the case when a fuel cell delivers current into an inverter that supplies a 10 kW load with an efficiency of 90%. The fuel cell will have to deliver 11.1 kW. At the worst-case low cell stack voltage of about 44 V, this implies dc current of

252 A from the stack. Current of this magnitude, while manageable, will require close attention to bus bar design and layout issues.

The University of Illinois at Urbana-Champaign (UIUC) Future Energy Challenge (FEC) team decided on a design approach that uses few conversion stages while maintaining excellent performance capabilities. Simplicity is important, and the design is intended to make the system work with an absolute minimum of other components. Although battery cost was not part of the formal scoring, our design keeps total system cost – inverter, batteries, and battery management – very low. To enhance long-term viability, our team added the requirement of input-output galvanic isolation to the design requirement set. The design as produced has two unique features:

- A new type of pulse-width-modulation (PWM) control is used to provide a simple control strategy for an ac-link inverter concept. This control makes isolation easy, and supports a cycloconversion approach to the inverter output stage.
- Simple nonlinear control strategies support high performance with minimal component complexity. The approach ensures a high-quality output with minimal cost for sensors and control.

We believe that this design achieves a significant advance in cost-performance for alternative energy conversion inverter systems.

## **2. Topology – general issues**

### *Requirements*

The conversion topology must achieve several specific engineering objectives:

- Current control for the fuel cell must be supported. Precise control of current with minimum low-frequency ripple is needed.
- The fuel-cell current control must be decoupled from the rest of the system. That is, the current must be fully controlled independent of the ac load.

- Energy storage must be provided to support decoupling between the fuel cell and the load, so rapid load changes do not affect the fuel cell.
- A high-quality two-port sinusoidal output is needed. The output must produce two separate 120 V ac 60 Hz supplies, in such a manner that the two supplies in tandem can be used to produce a single 240 V ac output. Low distortion is required.
- Load ratings of up to 10 kW (0 to 5 kW on each output leg) must be achieved.
- Other FEC performance requirements, such as no fuel-cell backfeed, fuel-cell turn-off capability, short-circuit capability, and robust output performance must be achieved.

*Alternatives*

From a conceptual viewpoint, there are two general approaches that can be taken to this inverter problem:

1. Convert the energy from the fuel cell into ac form, then step this up to produce the desired output. An example is given in Fig. 1. The trouble with this approach is that the transformer will have to be rated for the 60 Hz fundamental frequency of the output. The size and weight of a 10 kW transformer at 60 Hz are such that FEC requirements probably cannot be met this way. This is true even though the cost might be low.

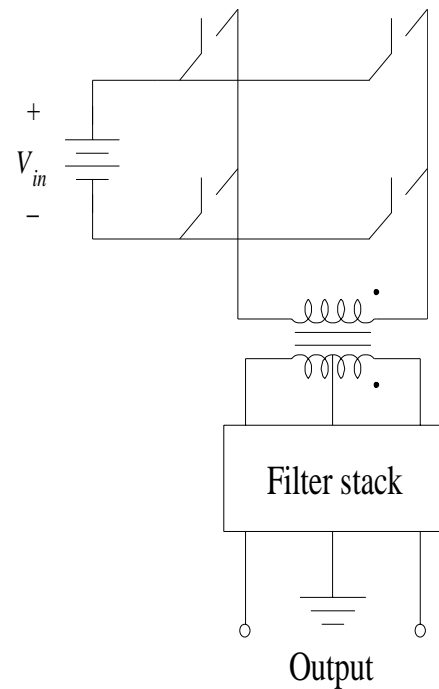


Figure 1. Inverter with 60 Hz link.

2. Use a dc-dc conversion approach to step up the voltage (perhaps at high frequency), then use a conventional inverter to produce the ac output. In concept, this approach can be treated as a conversion from dc to high-frequency ac, a rectification to high-voltage dc, and inversion to 60 Hz.

The proposed design actually uses a third approach, based on ac link cycloconversion methods.

This replaces the rectification stage and performs inversion directly, simplifying the system.

Cycloconversion techniques are rarely used because of the control complexity, problems with devices, and poor output harmonic characteristics. Our team decided that these limitations are not really fundamental: it should be possible to produce the desired output waveform directly from the ac link stage without the problems of a cycloconverter. We were able to identify a new way to perform pulse-width modulation (PWM) that actually produces a cycloconverter with a standard PWM output. A PWM output has the advantage of simple filtering and high-quality waveforms, although the losses are higher than in some types of inverters.

*Evaluation*

For the moment, let us rule out alternative 1 based on excessive weight, and look more

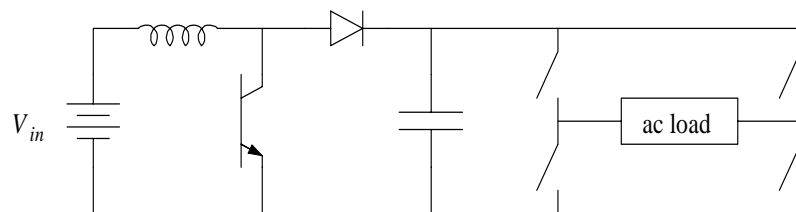


Figure 2. Boost/inverter cascade.

closely at alternative 2. In general terms, the conversion process can be treated as a cascade of a step-up from the fuel cell stack and a conventional inverter, as in Fig. 2. This is a boost converter cascaded with an inverter bridge. But what about the batteries? This arrangement does not provide operational decoupling between the fuel cell and the inverter. Although batteries can be added (in place of the capacitor in the center of the circuit), they would have to support full bus voltage – an expensive approach.

In addition, the boost gain needed for the circuit of Fig. 2 is extreme. A gain of more than 7 from input to output must be achieved at high power with high efficiency. Such extreme gains place severe requirements on the filter components, and seem unlikely to be practical.

We could treat the fuel cell and the batteries as two more or less independent inputs to the boost converter – in the form of a current-sourced forward converter. Fig. 3 shows a current-sourced converter that can meet the basic requirements. The fuel cell supplies one input port, and the batteries another. The general concept is that of a current-sourced forward converter, followed by a simple voltage-sourced inverter bridge.

The concept in Fig. 3 is viable, but has a number of challenges that prevent it from becoming a lost-cost solution. First, four significant magnetic elements are needed: two input-side inductors, the forward-converter transformer, and an

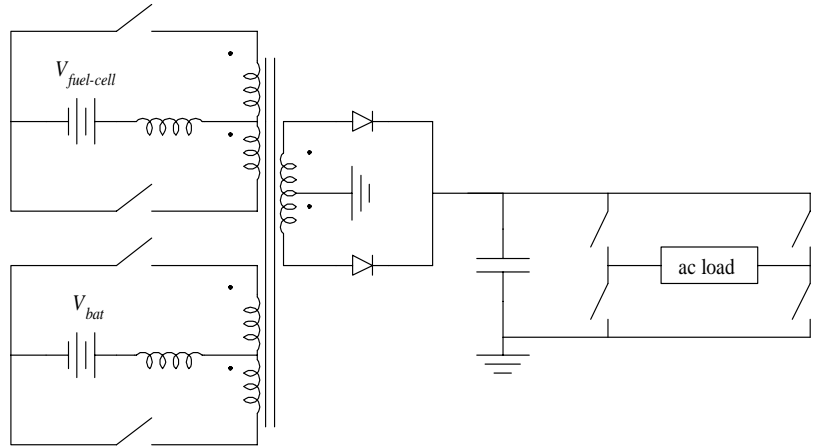


Figure 3. Dual-input forward converter/inverter cascade.

output-side filter inductor (inside the “ac load” block). Second, the battery conversion portion must be bidirectional to support both charge and discharge. The inverter bridge does not support dual output ports, although it permits either a voltage-sourced inverter approach or a PWM inverter control. An advantage of the approach is the redundancy of the fuel cell and batteries: operation can take place with just one source connected. Another advantage is high efficiency: the batteries do not have to act as an intermediate energy source if power can flow directly to the load.

The most significant issue in Fig. 3 is that of control decoupling. In principle, the battery current can be chosen to exactly cancel dynamics of the inverter load to ensure constant current draw from the fuel cell. In practice, it is hard to do this precisely. Since the fuel cell supplies the forward converter directly, any change in the ac-side current will alter the fuel-cell current unless control action is instant.

Another way to connect the batteries is shown in Fig. 4. This is the same as Fig. 3, except that the batteries have been moved to the forward-converter output bus. Fig. 4 is extremely simple and has considerable appeal, but from a system-level cost perspective it is flawed. The battery bus will need to have a nominal value of about 340 V, which requires series connection of 28 lead-acid batteries. This long series connection is not out of the question [3], but the charging of a long series string leads to imbalance problems [4]. There is one low-cost approach in the literature for battery balancing [5], although a much

more expensive approach [6] has been commercialized. In either case, it would be preferable to minimize the imbalance problem and avoid the cost of an extensive battery balancing network and wire harness.

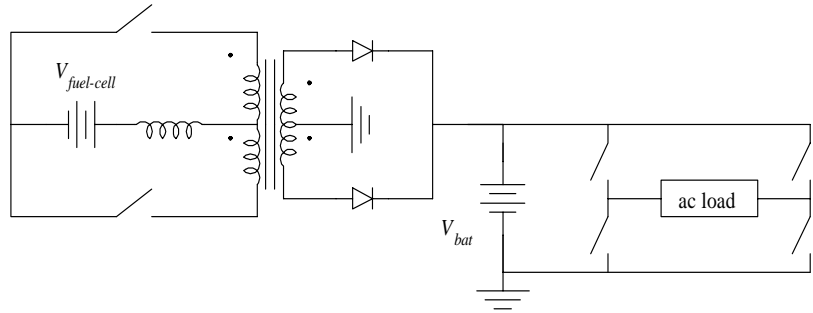


Figure 4. Forward converter driving batteries and inverter.

Fig. 5 shows a boost converter, followed by a voltage-sourced forward converter and inverter.

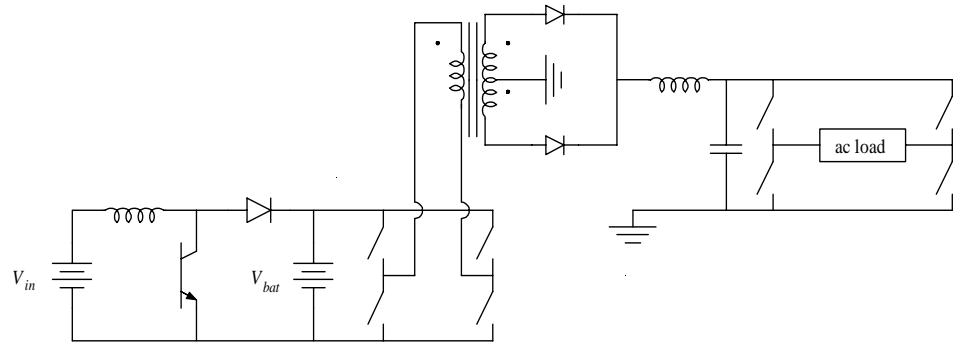


Figure 5. Three-stage converter: boost/forward/inverter.

A key advantage of this topology is decoupling of control: the boost converter can act to maintain the desired current from the fuel cell, independent of the forward converter action or of the inverter. There are two major troubles with this topology: First, the extra diode in the boost converter reduces efficiency compared to the two-port converter approach in Fig. 3. Second, this arrangement in effect adds an additional conversion stage – although the number of components has not changed much and in many ways Fig. 5 is about the same in terms of complexity as Fig. 3.

In Fig. 5, there are three sets of controls: the initial boost converter control, the forward converter control, and the inverter control. Furthermore, the power conversion blocks proceed from the current-sourced fuel-cell input, to the voltage-sourced battery bus, to a current-sourced output filter for the forward converter, to the voltage-sourced inverter. This stackup of sources can be reduced, since at least one source is redundant. Reduction of redundancy will eliminate a portion of the control as well as the extra stage. The concept is embodied in a high-frequency link arrangement, shown in Fig. 6. In this circuit, the

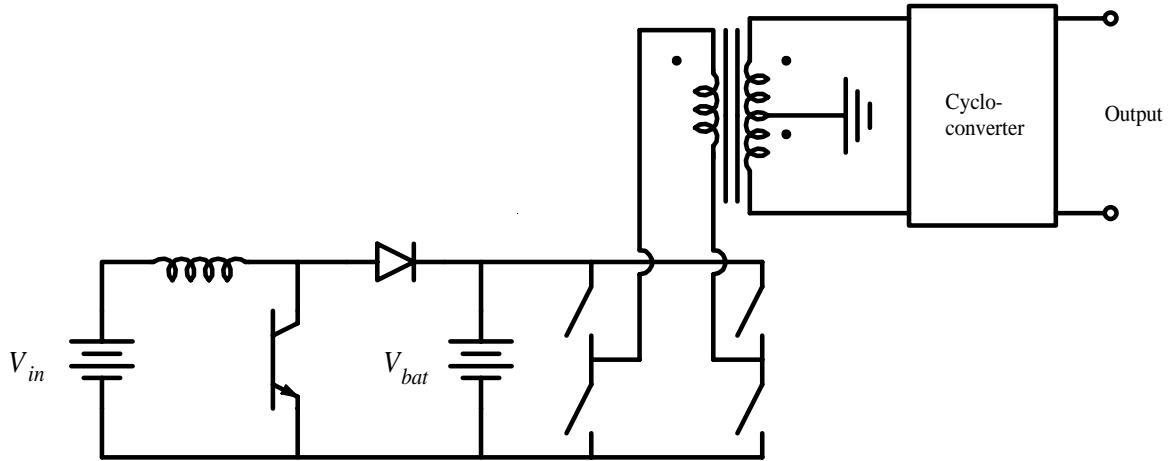


Figure 6. Boost converter, followed by ac link inverter and ac-ac converter for output.

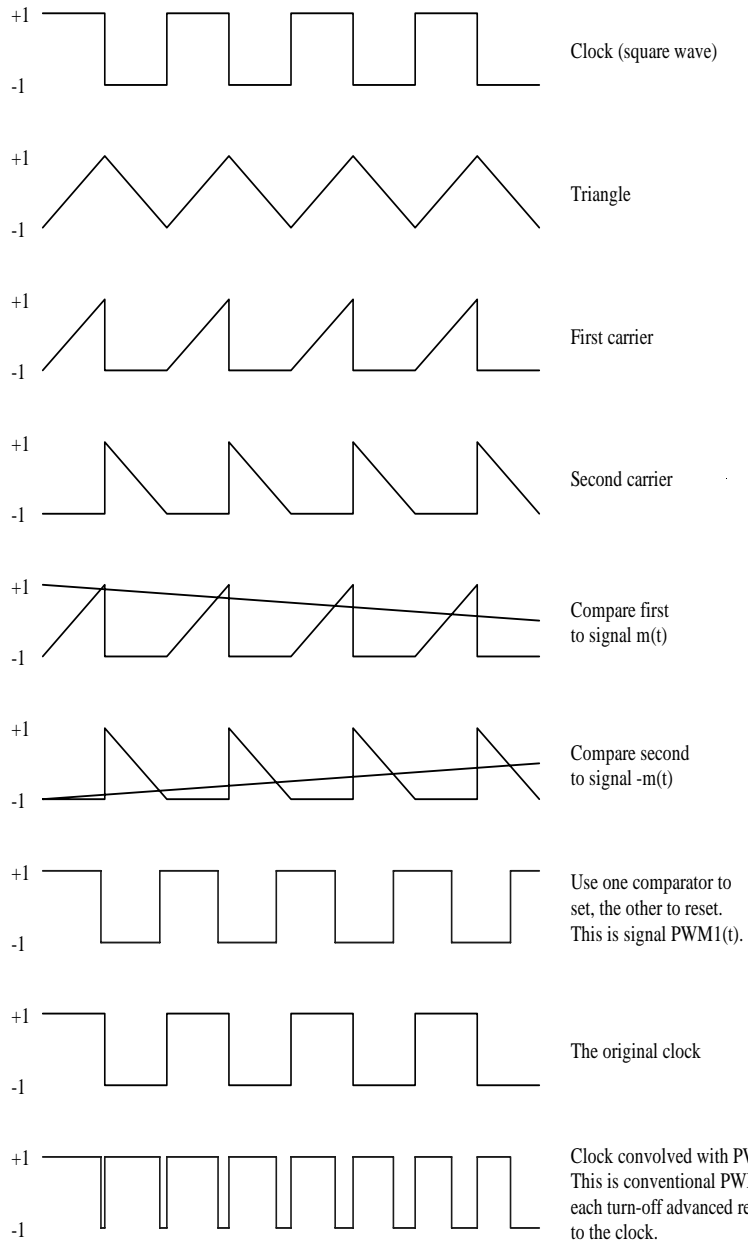
forward converter is replaced with a simple square-wave inverter which delivers a square-wave voltage to the output bus. The inverter is replaced with an ac-ac converter to deliver the 60 Hz output. In this sense, the ac link approach leads to a cycloconverter-type system, in which a square wave ac input is chopped to deliver the desired output.

#### *PWM Cycloconverter*

Cycloconverter circuits are generally held to produce substantial distortion, but is this an essential element? The answer is found in conventional PWM. In a conventional PWM inverter, a dc level is switched from positive to negative to deliver two-level output to a filter. If the switching frequency is much higher than the desired output frequency, filtering is straightforward, and a low-pass filter can recover the desired ac output. In principle, it should be possible to produce the *same waveform* as a conventional two-level PWM signal starting from a two-level square wave. This is the basis for our team's invention in inverter control: multi-carrier PWM. We refer to the resulting converter as a *PWM cycloconverter*.

In multi-carrier PWM, a triangle function or sawtooth is split into two separate carriers. Each is used to modulate the desired sinusoidal waveform. When the resulting PWM signals are combined, the result can be selected to avoid low-frequency signal while preserving the underlying output. The concept is shown in Fig. 7. Multi-carrier PWM has several key advantages in the context of low-cost inverters:

- It is easy to generate multi-carrier PWM. Just as conventional PWM can be created with a sine-triangle combination into a comparator, so multi-carrier PWM can be generated with a bit of logic plus comparators. It is about as easy to generate multi-carrier PWM in digital form as for conventional PWM.



- The resulting waveforms are ideal for ac links. In the selected case, for example, the waveforms are square waves with duty

Figure 7. One example of PWM based on two carriers.

ratio close to 50% at the

switching frequency. They can be delivered to the output switching devices via small transformers without regard to low-frequency saturation effects.

- A filter stage is eliminated. There are now just three primary magnetic elements: the input interface to minimize fuel cell ripple, the ac link transformer, and the output filter inductor.
- The topology extends well to extremely high power levels, since the cycloconverter method

supports the use of SCRs as output switching devices.

An important disadvantage is that each output switch must be bilateral, in the sense that each must carry ac current and block ac voltage. This produces higher output voltage drop than single devices would, but it has the advantage of reducing the individual device current ratings. The increased output drop will be addressed through the use of a half-bridge output connection arrangement.

### 3. Topology -- specifics

#### *The Per-Unit System*

The overall topology is shown in Fig. 8. For convenience, we start by defining a per-unit system for the conversion topology [7]. At the input, 48 V serves as a natural voltage base, with 10 kW as the

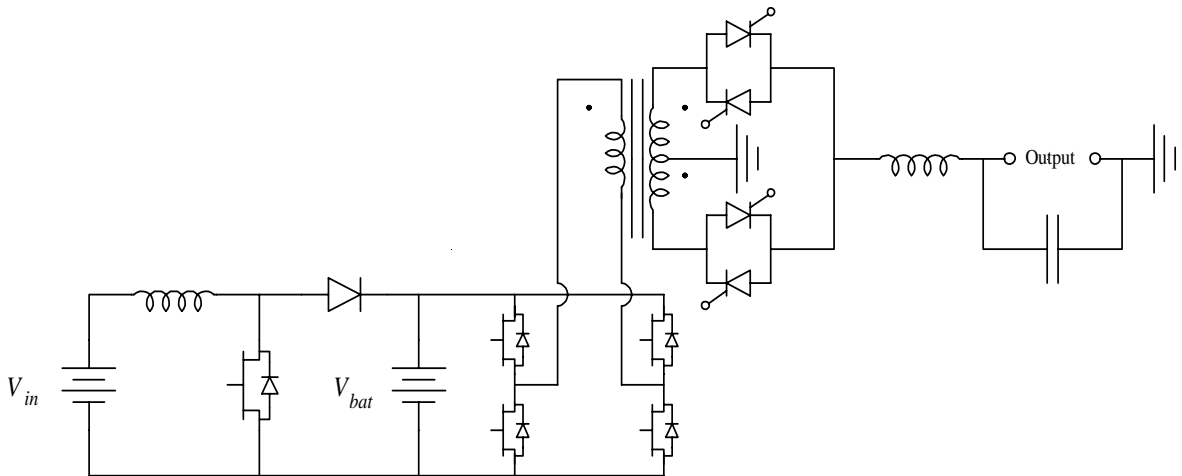


Figure 8. Proposed ac link converter with boost input stage. Only one of the two ac outputs is shown.

power base. The current base becomes 208.3 A. The effective impedance base  $V_{base}/I_{base}$  is  $R_{base} = 0.230 \Omega$ . At the output, the power base is still 10 kW, but the voltage base is 240 V. The current base becomes 41.7 A, and the impedance base becomes  $2.88 \Omega$ . It is not quite possible to infer a transformer ratio, as in an ac system, since the input base is dc and the output is ac. Nevertheless, the per-unit approach will help with identification of ripple levels, filter element values, and other important converter attributes. Notice that efficiency on the order of 90% suggests losses not to exceed 1.11 kW at full load.

### *Switching frequency and other baseline assumptions*

For a 10 kW design, conventional motor drive systems imply that 10 to 20 kHz is a reasonable switching frequency range. In this PWM cycloconverter topology, a lower frequency might be needed to support SCRs as output devices. For the purposes of initial design, let us assume a switching frequency of 10 kHz and a period of 100  $\mu$ s. Other assumptions will be that 90% efficiency is in fact achieved, that the fuel cell stack operates within its control range of 42 V to 60 V, and that individual switches can be characterized as 1 V forward drops when on.

### *Boost converter*

The losses in a boost converter are substantial in the two switches and in the parasitic resistance of the inductor. If the switches really are fixed forward drops, the losses are independent of duty ratio. Our experience with solar cells, however, suggests that low duty ratios for the active switch tend to yield better efficiency. One reason is that commutation loss in the devices is proportional to output voltage. A second reason is that low-drop Schottky diodes can be used for the passive switch.

Since the input topology is that of a boost converter and the output voltage should be low, we seek a battery bus voltage that is just slightly higher than the nominal 48 V fuel cell voltage. The choice of a 60 V battery bus has been made by our team, for several reasons:

1. If a 48 V battery is used, and it is partially discharged, there are situations in which the fuel cell voltage can exceed the battery voltage. In these cases, the batteries could continue to draw current from the cell stack even if the system requests complete shutoff.
2. A 60 V battery, operating under normal circumstances, will permit complete shutoff.
3. In the event of failure of the active switch, the fuel stack could still be used to supply power, albeit at reduced rate. This would help prevent failure of the batteries from overdischarge if the primary input active switch fails. This single-failure limited function mode should enhance reliability.
4. The rules allow battery energy of 500 W-hr for a 1500 W unit, which scales to 3.33 kW-hr for a 10 kW

unit. The battery size at 60 V would be 55 A-hr – just in the range of low-cost car batteries. This would be a strong benefit in keeping the system cost low.

5. With just five batteries in series, the charge management process in [5] would be inexpensive and easy to use. It is expected that the batteries would last for several years with this accessory.
6. A 72 V battery stack could also be used, but would not permit the single-switch failure limited-function mode. Even if the fuel cell is permitted to reach its full open-circuit voltage of 72 V, a five-battery stack would see no more than 14.4 V per battery, which is a safe level for VRLA batteries over time frames of a few days or even longer.

For the choice of inductor, let us assume a 60 V battery stack and 48 V fuel cell stack. The converter nominal duty ratio for the active switch, based on [8], would be  $D_1 = 1 - 48/60 = 0.2$ , and the diode duty ratio would be about 0.8. The boost converter must take power from the fuel cell, with controlled (slowly varying) current and deliver it, via the battery bus, to the ac link. With 90% efficiency, the input current will be 1.11 per unit. At a switching frequency of 10 kHz, the ripple specification permits large ripple. However, ripple in a boost converter is an absolute number rather than a load-dependent number. Since the specification limits ripple down to 10% load, a design that will meet requirements at 10% load should be suitable for the entire range. According to the specification, ripple of 60% peak-to-peak is permitted. Based on 10% load and 90% efficiency, this allows 6.67% per-unit ripple current. With a ripple current of 6.67% and a duty ratio of 20%, the inductor value needed at light load is 60  $\mu\text{H}$ .

Switch ratings need to be 1.11 per unit current, and about 75 V for the maximum possible battery voltage, plus headroom for commutation. In principle, 100 V devices would be sufficient, although 150 V devices might be preferred for reliability. We have selected 100 V devices with ratings of 250 A for the boost converter switches.

#### *Ac link system*

In the PWM cycloconverter method, the ac link voltage can be either a simple two-level square-

wave or a three-level waveform with short dead times. Since the battery bus is subject to variation, possibly beyond that permitted for ac voltage regulation in the requirements, a simple sensorless current-mode flux controller [9] is used to maintain a fixed volt-second pulse contribution at the ac link input. This controller operates open-loop with respect to the output, such that no feedback across the isolation is needed. It compensates for battery voltage variation. The ac link input is drawn as a full-bridge topology, as is conventional for currents on the order of 200A. In actual implementation, there could be advantages (based on safety and cost) to splitting the fuel cell and battery buses, say to a bipolar  $\pm 36$  V connection. Since the fuel cell stack itself is not available to us, we elect a bridge arrangement for reliability.

The ac link output in Fig. 8 looks like a half-bridge, but this is misleading because of the dual-port nature of the output. Only one of the two outputs was shown for clarity. In a sense, the actual two-port output is more reminiscent of a “center-tapped bridge,” and does not suffer from underutilization of material if the two output legs are balanced. If they are unbalanced, operation is unaffected. The output voltage must be sufficient to create a dual  $\pm 170$  V to 180 V output to provide sufficient voltage for the cycloconversion process. Based on the bridge input design, this suggests a voltage ratio of 1:3 for each half-winding set in the transformer. The core must be selected to handle 60 V for 50  $\mu$ s on each input half-winding, or 0.003 V-s for the winding. Copper must be large enough to handle 1 per-unit current pulses.

#### **4. Filtering**

##### *Input filter inductor*

The input and output filters are the primary filter elements in the system. The initial design uses conventional discrete components. It is expected that the final design will make use of coupled-inductor filter techniques [10]. For inductors, we intend to use powdered iron cores. The material is well-suited to 10 kHz switching levels, and is low in cost. Even large cores can be obtained for a few dollars. Consider a toroidal T650-26 powdered iron core from Micrometals. This core has inductance of 434 nH/turn<sup>2</sup>, and

cross-section area of  $18.4 \text{ cm}^2$ . The input inductor carries 230 A nominal, so a 250 A rating should be sufficient. To keep flux levels below 1 T, magnetic circuit analysis permits no more than 17 turns. At 17 turns, the core should provide inductance of  $125 \mu\text{H}$ . A worst-case analysis shows that this is more than sufficient to meet the ripple requirements. At heavy load, as the inductance drops off, it remains sufficient.

It is hard to wind a large core with large wire to meet a 250 A rating. We elected to wrap the core with conventional braid, since ribbon was not available. It is easy to double or triple the braid to obtain high current ratings. Fig. 9 shows the core for the 10 kW unit input filter (boost converter inductor). The wire size is about  $63 \text{ mm}^2$ , which carries 250 A with current density of about  $400 \text{ A/cm}^2$  – probably acceptable given the large core and open construction.

In the final design, a second winding of about #12 gauge will be added to provide coupled-inductor filter capability at little extra cost. This supports the addition of a filter capacitor – sized to handle ripple current of about 12 A – to further reduce the input ripple.



Figure 9. Input inductor for 10 kW inverter system.

Notice that the system design has no inrush current, and also that the fuel cell is fully buffered from the output. We expect little or no ripple at 60 Hz or 120 Hz.

#### *Output filter*

The output filter design is conventional in PWM inverter practice. The objective is to block as much as possible at switching frequency while passing as much as possible at 60 Hz. The base impedance

is  $2.88 \Omega$ , which provides a basis for design. Consider a simple LC filter, with series L on the load and parallel C across it. We want  $X_{L(60)} = 377L$  to be much less than  $2.88 \Omega$ , and  $X_{L(10000)} = 62830L$  to be much greater than this. The choice  $X_L = 2.88 \Omega$  at 600 Hz is a good compromise. This yields  $L = 760 \mu\text{H}$ . The current rating should be the peak value of about 58 A. This combination can be accomplished with 38 turns of wire on two T400-26D powdered iron cores. A larger single core can be used instead.

The parallel capacitor needs to have reactive impedance much less than  $2.88 \Omega$  at 60 Hz and much larger at 10 kHz. Once again, choose about 600 Hz as the value for  $2.88 \Omega$ . The result is  $C = 92 \mu\text{F}$ . The combination resonates at 600 Hz. Simulations suggest that this compromise works well. A coupled inductor filter may be added to the output inductor in the final design to steer some of the ripple frequency directly to ground.

#### *EMI and Other Filter Issues*

The bulk of the noise is generated in and between the input and output filters. The transformer design will be especially important for EMI minimization. Tight coupling and close winding will be needed. We are contemplating the use of Faraday shielding within the transformer.

### **5. General tradeoffs and auxiliary design issues**

#### *Battery sizing*

According to the FEC specifications, the fuel cell requires up to 90 s to come to full power when starting. Let us assume that when the user activates the inverter, power is available immediately. The worst-case situation would be for the inverter to consume 1 per unit power during 90 s when fuel cell power is not available. With 11.1 kW input, this corresponds to 278 W-hr of storage. This value (1 MJ) is too large for capacitor storage, so batteries will be required. However, at these extreme rates, batteries are not very efficient, so a significant oversizing will be needed.

In keeping with the topology, a nominal 60 V battery (five 12 V units in series) will be used. Fig. 10 shows the discharge behavior of a 32 A-hr valve-regulated lead-acid (VRLA) battery pack, based on manufacturer data. The curve shows measured data for discharge tests ranging from 5 min to 6 hr. It follows an approximate log-log characteristic. The dotted line shows a model, which suggests that the power capability is a function of discharge time,

$$P = 1230t^{-0.7} \quad (1)$$

with  $P$  in watts and  $t$  in hours. For 1.5 min, or 0.025 hr, this suggests a power of 16.2 kW – about 50% headroom over the needed power. The extra headroom is important, since we do not want the batteries to become fully discharged during startup. If they are fully discharged, there is no extra storage available to accommodate load changes after startup is completed. Therefore, 32 A-hr appears to be the correct size.

A capacity of 32 A-hr in a VRLA battery is an especially useful choice. This corresponds well to the industry-standard U1 battery size, common in telecommunications, uninterruptible power supplies (UPSs) and other applications. Many manufacturers produce such a battery, such as Johnson Controls,

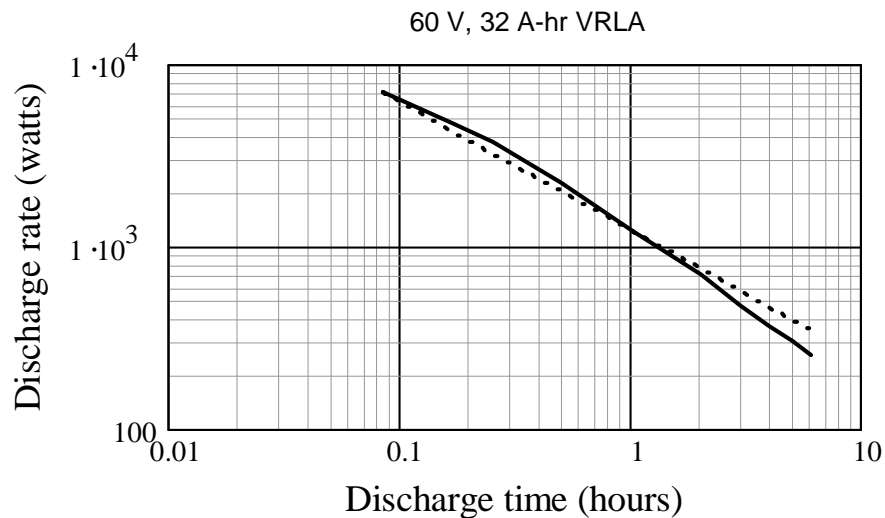


Figure 10. Manufacturer's discharge data for 32 A-hr battery set. Solid: measured. Dotted: logarithmic model. (Based on data sheets for the Johnson Controls UPS 12-95 VRLA battery.)

Panasonic, Yuasa, and others. Other manufacturers, such as Hawker Energy, produce an equivalent in a slightly different package. U1 units are low in cost because of strong competition. Fast-discharge designs based on UPS requirements are readily available.

#### *Battery management*

Most of the battery charge management issues are addressed by the control, especially the boost converter control. This is discussed below. In addition, a series string brings with it the problem of equalization: the batteries in the string must be kept balanced. This problem is not always appreciated, but is known to be an essential aspect of VRLA battery application [4]. In our case, we intend to use an invention published by our group in 1997 as the basis for the process [11]. The advantage is high performance at low cost. Prototypes so far are less than 10% of battery cost. This is a small price to gain substantial reliability improvement.

#### *Auxiliary Power*

The system requires power for control and operation. This power must be available before other functions can take place. In this system, control power is a relatively simple issue since the batteries are available. Power could have been provided from a separate dc-dc converter, but this was thought to be an unnecessary cost.

At startup, auxiliary power is supplied temporarily from the batteries until all functions are in action. After that, two small auxiliary windings on the main transformer are rectified to provide continuous dc-dc conversion power. A small power switch controls both sources, so control power can be removed quickly and unambiguously when shutdown is desired. Control power is regulated close to the desired +5 V and +12 V levels. For battery power, a series pass transistor is needed. Since linear regulators in general are not rated for more than 35 V input, a separate NPN pass transistor is used. This transistor should not need to operate for more than a few seconds, so thermal issues in this part of the design are minor. A simple diode-or approach cuts out battery power when transformer power becomes available.

With a 5% tolerance on the 12 V Zener, the diode arrangement will function as long as the transformer produces a voltage higher than about 12.0 V. The transformer turns are designed for about 15 V, so problems are avoided. The arrangement appears in Fig. 11.

## 6. Control

### *Control objectives*

The control system for this inverter is intended to be simple, and takes advantage of the fixed-output nature of the inverter. It also takes advantage of the fundamental action of the converter stages. For example, it is necessary and sufficient to turn off the transistor in the boost converter to shut off power drawn from the fuel

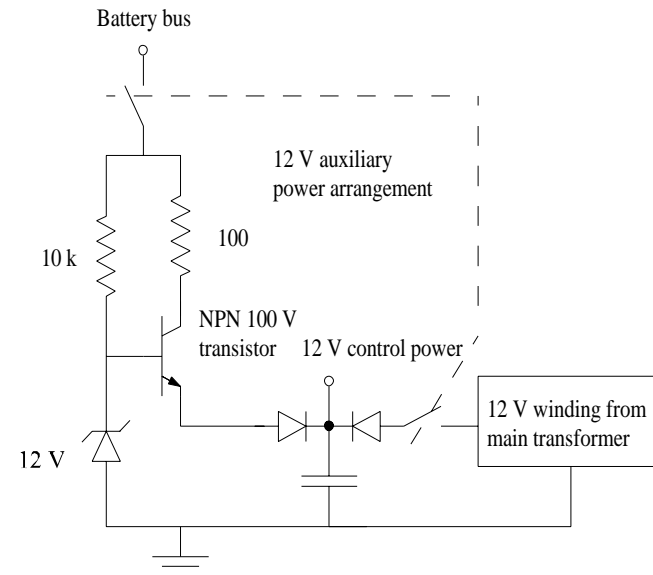


Figure 11. 12 V auxiliary power connections.

cell. It is also sufficient to use current control based on the input inductor to obtain the intended fuel cell current level. Our controller has few components. Each set of switches acts open-loop in the sense that each can have a separate control.

Simple logic provide most of the basic control functions. For the final design, we intend to use a simple 68HC12 microprocessor for most functions. This processor has plenty of computational power at very low cost. Low-cost DSPs are also an alternative, although their computational capability is considerably more than is needed in this design.

### *Boost converter control*

The boost converter is intended primarily to enforce current control from the fuel cell. The boost controller uses a fixed-frequency boundary technique [12] to enforce both an input current limit and a battery voltage limit simultaneously. If battery voltage reaches its upper limit, the boost converter begins

to shut down. The boundary controller is enabled only if the fuel cell voltage is above 42 V and the “fuel cell ready” digital input is high. If either signal is flagged, switching stops immediately.

Current reference enforcement is a closed-loop operation based on the “available current” command from the fuel cell. Current is sensed through a low-resistance shunt or current transformer when the active switch is on. Average current when on is compared with available current. An integral controller keeps these values identical, limited only by the accuracy of the shunt measurement.

The boundary controller works as follows:

- There is a primary 10 kHz system clock. If fuel cell voltage is above 42 V and the battery voltage is not too high, the active switch turns on at the start of a cycle.
- The current climbs until it reaches a reference value, and shuts off early if the voltage becomes too high. The duty ratio is not allowed to exceed 50%, so the switch turns off if the 50% point is reached without contact with the boundary.
- Formally, the boundary used for control has two segments:
  1. A current limit segment, defined by the available current from the fuel cell.
  2. A voltage limit segment, defined by a line connecting the maximum current (252 A) and a desired battery voltage (such as 66 V) to a point at the absolute maximum allowed battery voltage (73 V) and 0 A. This way, as the battery becomes fully charged, the boundary controller gradually backs off the battery current to complete the charge cycle.

This simple combination enforces the limits with minimal effort.

How is the reference current chosen? The intention is to keep the batteries full over a long period of time. This can be enforced, for example, by maintaining the average battery current to a small positive value over indefinite time. In our system, the fuel cell is asked to provide that current that enforces 1 A net battery current on the basis of a one minute moving average. In other words, the average current drawn by the transformer is evaluated continuously, and the fuel cell is asked to provide this value plus 1 A as its

command value. In case 1 A is not enough, an outer voltage loop allows the converter to request more as the average battery voltage falls below about 62 V. This loop uses a slow integral control, so the requested current rises gradually as average voltage falls. In the long run, this approach will keep the batteries fully charged on average.

#### *Ac link transformer control*

The ac link uses 10 kHz switching from the same clock as the boost converter. The control is a simple phase-shifted bridge control, set to impose a specific volt-second product on the transformer primary. The system is configured to work with no change in performance for battery bus voltages between 58 V and 72 V. The operation is direct: based on 50% duty at 58 V, the controller applies  $58 \text{ V} \times 50 \mu\text{s} = 2900 \mu\text{V}\cdot\text{s}$  in one configuration, then  $-2900 \mu\text{V}\cdot\text{s}$  in the other. Any extra time is dead time, spread between the two half cycles. Thus if the battery voltage is 72 V, the product  $2900 \mu\text{V}\cdot\text{s}$  requires a duty ratio of 40.3%. The transformer flux change is always well-defined under this control. This square wave is present whenever the converter power is on.

Gate driving and snubbing issues are relatively simple for the ac link converter. The leakage inductance is always provided with a current path by virtue of the bridge, although we do intend to provide small turn-off snubbers to improve losses. We have procured a gate drive transformer that can send signals to all four bridge switches at once. In this part of the circuit, each switch needs to carry about 170 A when on, but the duty ratio does not exceed 50%. Therefore a part with a continuous rating of 170 A should be sufficient for the work (or three 60 A parts in parallel). The voltage should not exceed 100 V, although a rating of 150 V or 200 V is probably a more reliable choice.

#### *PWM Cycloconverter*

The waveform at the bottom of Fig. 7 demonstrates that a multi-carrier PWM approach can reconstruct a two-level PWM waveform given a square wave input. The gate control signal produced in Fig. 7 shows phase advance: the turn-on point always precedes the rising edge of the square wave. If the

carrier is split in the opposite fashion, a phase delay gate control is produced. The end result is that of a cycloconverter: Use phase delay with the positive-direction SCRs when the load current is positive, and use phase advance with the negative SCRs when current is negative. Simulation studies confirm that the method works as intended.

The PWM cycloconverter supports direct conversion for a square wave – a concept that has been previously published [13]. The new aspect is that multi-carrier PWM results in a conventional PWM signal, with the same control and harmonic properties. This is a big advantage. Output adjustment takes place simply by comparing a reference sine wave with portions of a triangle. The waveform construction allows even a low-end microprocessor, such as the 68HC12, to carry out the job. If SCRs are used, then the gate drives are supported entirely by pulse transformers. However, this is not limiting. IGBTs or other devices can also be used to form the necessary bilateral switches. In this case, the gate drive waveforms have a duty ratio close to 50% at all times, and are convenient to couple with the switches by transformer. The PWM signals will support both outputs of the inverter. More evidence of operation and effectiveness is given in the Simulation section.

The only complication with SCRs is the need to sense the output current polarity. To ensure a reliable sensing operation, a small preload (about 20 W for lamps and fans) will be connected internally to the inverter output. As long as this current can be sensed with reasonable accuracy, the sign can be determined and the converter will function.

#### *Short circuit protection*

Since output current polarity is needed for cycloconverter control, a representation of the current will also be available for protection. If the output current rises too high (defined as more than 10% about the rated peak) or if the output current derivative is too high (defined in terms of the expected derivative at full load with low power factor), current can be shut off. The only complication is to avoid false tripping when a high-inrush load is applied intentionally. In this case, SCRs become especially valuable as the

output devices. They can handle high  $I^2t$  loads without failure. We can make the decision to support a short-term overload (such as might occur with a motor or large power supply) before tripping. In fact, the weakest link is probably the IGBT bridge at the ac link input. For the initial design, we intend to be conservative and trip when the current exceeds 110% of the allowed peak.

## 7. Simulation

Extensive simulation in PSPICE, Matlab, and even in simple BASIC programs has been carried out. In addition, experimental work has been conducted by the team on various stages of the converter. Two of our team members also prepared an active fuel cell emulator – a computer-controlled power supply that shows the V-I behavior of a loaded fuel cell.

Fig. 12 shows output voltage and input current for the 1500 W scaled complete converter in PSPICE. The converter is running entirely open-loop in this graph, since the PSPICE student version cannot handle enough complexity for closed-loop control. The output shows minimal distortion, and the

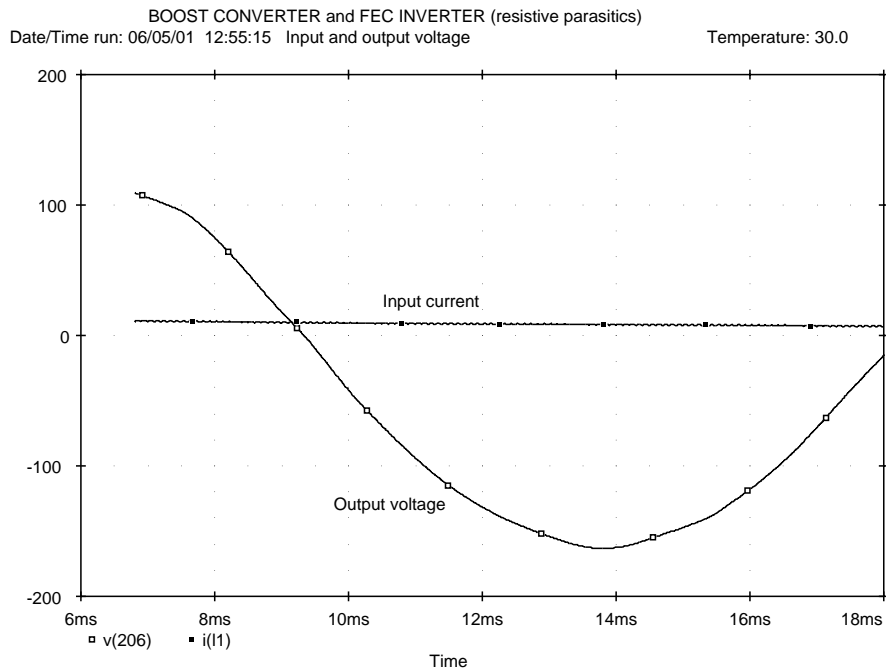


Figure 12. Complete 1500 W converter, simulated input and output.

input current ripple at 60 Hz is too low to measure. This plot has been generated with all parts of the system, boost, ac link, and cycloconverter, in normal operation with filters in place.

Fig. 13 shows Matlab results normalized to a battery voltage of 58 V. This figure confirms that the simple volt-second control at the ac link does in fact result in an output that is proportional to the modulating function. In this case, the system runs first with 50% duty and 58 V input (the solid trace). The sine wave is selected to produce the desired 1 p.u. output. Then the system runs with 72 V at 40% duty (the dotted trace) and the same sine wave reference. The results are very close.

We have also performed extensive analysis on the multi-carrier PWM approach, too lengthy to provide here. The method shows great promise for simplifying the application of ac link converters.

### 8. 1500 W Prototype

For the 1500 W prototype, the most significant change is that of the base units. The per-unit design does not change, although the values differ. The system has the same controls and the same level of complexity.

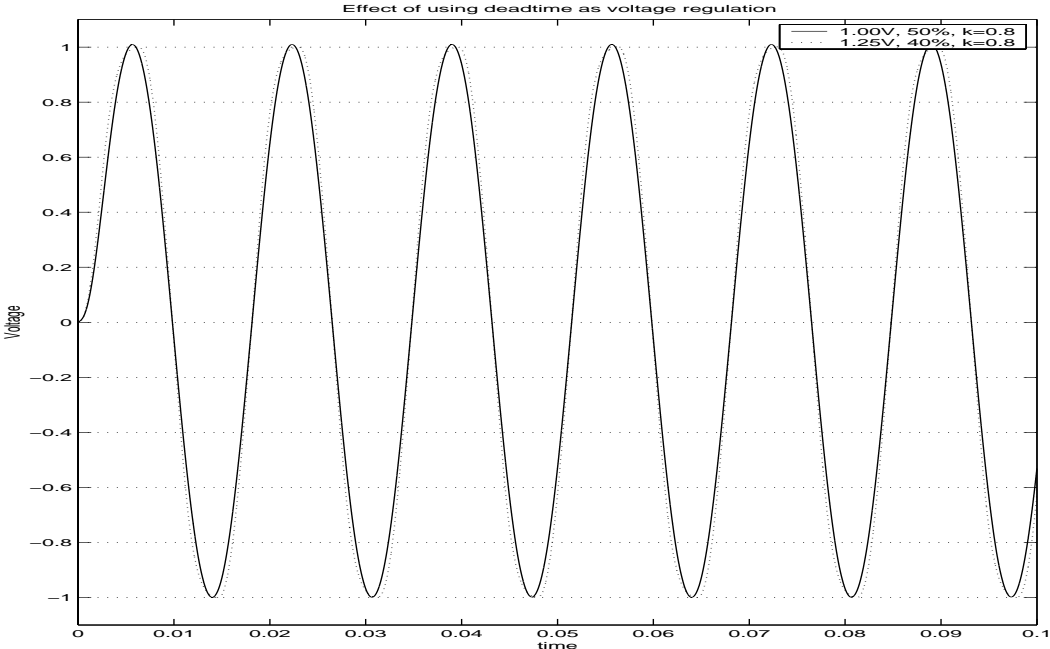


Figure 13. Converter output for two different battery voltages.

Details: The boost converter inductor is wound on a smaller core, and has  $L = 1120 \mu\text{H}$ . The filter elements are selected based on a  $19.2 \Omega$  base, which gives  $L = 5 \text{ mH}$  and  $C = 14 \mu\text{F}$  for the output filter. Magnetics and devices are physically smaller, but the control is identical. Batteries are also smaller. Our pack uses five 7 A-hr batteries, to provide total storage of up to 420 W-hr. This is within the FEC specification limit. We will retain the use of equalizers.

## 9. Cost Analysis

We believe that our design provides at least three ways in which substantial costs have been saved:

1. The PWM cycloconverter approach keeps the number of stages low and allows robust SCRs to be used in the output stage. It seems likely that an ac link will be needed in the long run to address safety standards without the heavy weight of 60 Hz magnetics. Since the new approach supports PWM waveform performance with an isolated ac link, it is likely to have value as standards become better defined.
2. The control is extremely simple. With few sensors and not much to do, low-cost microcontrollers can manage the whole system. We strongly believe that our controller costs will be far below those assigned in the scoring spreadsheet.
3. Our use of batteries provides a low-cost solution. The 10 kW design uses five commodity U1-size VRLA batteries. Our low-cost equalization system will allow them to be used in this aggressive application without compromising their cycle life and operating life.

We believe that all three of these aspects are special contributions that bring costs below what would be expected via the spreadsheet. There is good reason to believe that the entire system can be constructed for well under \$500, *with batteries*.

Spreadsheet results show a higher value, but only because of overly conservative magnetic component cost estimates. When we substitute direct cost estimates for spreadsheet point values, the total

cost of our design comes to about \$480 – even with the spreadsheet estimate of 20% for control cost, which is very high compared to our expected result.

## **10. Education and team**

The College of Engineering at the University of Illinois has been strongly supportive of student team activities, particularly integrated teams such as that intended to carry out the FEC. This past year, our students participated through their Senior Design Course, a required senior-level capstone course. Students in groups of two or three carries out some of the key design efforts of the Challenge.

Some students also participated through our undergraduate Power Electronics Laboratory Course. This unusual course, which has been in the curriculum for twelve years, requires a design project as part of the activities. A few of the students attempted 60 Hz inverters as part of their work.

These efforts have been strongly successful. In the 2001-2002 school year, our College will be trying a new 6-credit-hour interdisciplinary design course explicitly for large student projects. A student-built satellite will be the first activity. This is an outgrowth of our many years of Department of Energy projects, beginning with the Hybrid Electric Vehicle Program in 1992 and carrying through to the 2001 Future Energy Challenge.

This year, our student team was relatively small. Robert Balog served as a graduate Team Advisor, and assisted each group of student with the details of their design and experimental work. He has carried out the Matlab simulations as well.

## **11. Operating Instructions**

The system is simple to connect and use. To operate it:

- Turn both the power and inverter switches off.
- Connect the batteries and the fuel cell. Be sure polarities are correct.

- Connect the fuel cell control wires.
- Inspect connections to be sure they are correct and complete.

When the arrangement is ready, to start the system, the user must turn on two switches (in any order):

1. The power switch. This is the switch shown in Fig. 11. It energizes the controls, and of course the system will not function with it off.
2. The “inverter enable” switch. This turns on the SCRs in the output stage and begins the supply of power. Power will continue to be delivered until either the battery voltage falls below a limit value or until either switch is turned off.

When both are on, normal operation begins. A signal is sent to the fuel cell requesting power.

#### *Indicator lights*

There are four indicator lights. From left to right:

- Power. Shows that 12 V and 5 V power are functioning.
- Battery indicator. Shows that battery voltage is above the low limit.
- Fuel cell indicator. Shows that the boost converter is active and that the fuel cell is supplying power.
- Output. Shows that the inverter output is active.

In normal operation, when the unit is started the first two lights will turn on. If no problems are encountered, the output light will turn on once the inverter is activated. After the 90s initial transient, the fuel cell light should turn on.

#### *Troubleshooting*

If any light is off, a problem has occurred.

- Output light off: a fault has been encountered. To reset, turn off both switches, check for problems, then restore power.
- Fuel cell light is off: fuel cell is still in startup mode, or a fuel-cell control fault has been flagged.

- Battery light is off: batteries are too low for normal operation. To correct this, operate the unit for about 30 min with fuel cells on but the inverter switch off.
- Power light is off: unless the switch is off, an internal problem such as a component failure or blown fuse has occurred. Cycle power. If the problem remains after fuses have been checked, a service call may be required.

## 12. References

- [1] Fuel cells, *IEEE Spectrum*. June 2001.
- [2] P. T. Krein, "Tricks of the Trade: Simple Solar Cell Models," *IEEE Power Electronics Society Newsletter*, April 2001.
- [3] R. D. Brost, "Performance of valve-regulated lead-acid batteries in EV1 extended series strings," in *Proc. 13<sup>th</sup> Annual Battery Conf. On Applications and Advances*, 1998, pp. 25-29.
- [4] S. West, P. T. Krein, "Equalization of valve-regulated lead-acid batteries: issues and life test results," in *Proc. IEEE Int'l Telecommunications Energy Conf.*, 2000, pp. 439-446.
- [5] C. Pascual, P. T. Krein, "Switched capacitor system for automatic series battery equalization," in *Proc. IEEE Applied Power Electronics Conf.*, 1997, pp. 848-854.
- [6] N. H. Kutkut, D. M. Divan, D. W. Novotny, "Charge equalization of series connected battery strings," *IEEE Trans. Industry Applications*, vol. 31, no. 3, pp. 562-568, May 1994.
- [7] R. D. Shultz, R. A. Smith, *Introduction to Electric Power Engineering*. New York: Harper & Row, 1985.
- [8] P. T. Krein, *Elements of Power Electronics*. New York: Oxford University Press, 1998.
- [9] P. Midya, P. T. Krein, M. Greuel, "Sensorless current mode control -- an observer-based technique for dc-dc converters," *IEEE Trans. Power Electronics*, vol. 16, July 2001.

- [10] R. Balog, P. T. Krein, D. Hamill, "Coupled inductors -- a basic filter building block," in *Proc. Electrical Manufacturing and Coil Winding Ass'n.*, 2000, pp. 217-278.
- [11] C. Pascual, P. T. Krein, "Switched capacitor system for automatic series battery equalization," U. S. Patent 5,710,504, January 1998.
- [12] P. T. Krein, *Elements of Power Electronics*. New York: Oxford University Press, 1998, Chapter 17.
- [13] M. Matsui, M. Nagai, M. Mochizuki, A. Nabae, "High-frequency link dc/ac converter with suppressed voltage clamp circuits – naturally commutated phase angle control with self turn-off devices," *IEEE Trans. Industry Applications*, vol. 32, no. 2, pp. 293-300, 1996.

**You have reached the end  
of this final report.**

**Use the button below to  
return to the Main Document**